International Journal of Pharmaceutics 422 (2012) 479–488

Contents lists available at SciVerse ScienceDirect

International Journal of Pharmaceutics

journal homepage: www.elsevier.com/locate/ijpharm

Pharmaceutical Nanotechnology

Mathematical modelling of the transport of hydroxypropyl-β-cyclodextrin inclusion complexes of ranitidine hydrochloride and furosemide loaded chitosan nanoparticles across a Caco-2 cell monolayer

Armin Sadighi[a], S.N. Ostad[b], S.M. Rezayat[a,c], M. Foroutan[d], M.A. Faramarzi[e], F.A. Dorkoosh[f,*]

[a] Department of Medical Nanotechnology, School of Advanced Medical Technologies, Tehran University of Medical Sciences, Tehran, Iran
[b] Department of Pharmacology and Toxicology, Faculty of Pharmacy, Tehran University of Medical Sciences, Tehran, Iran
[c] Pharmaceutical Sciences Branch, Islamic Azad University, Tehran, Iran
[d] Department of Physical Chemistry, Faculty of Chemistry, College of Science, University of Tehran, Tehran, Iran
[e] Department of Pharmaceutical Biotechnology, Faculty of Pharmacy and Biotechnology Research Center, Tehran University of Medical Sciences, Tehran, Iran
[f] Department of Pharmaceutics, Faculty of Pharmacy, Tehran University of Medical Sciences, P.O. Box 1439956131, Tehran 14174, Iran

ARTICLE INFO

Article history:
Received 23 July 2011
Received in revised form 14 October 2011
Accepted 6 November 2011
Available online 11 November 2011

Keywords:
Chitosan nanoparticles
Furosemide
Ranitidine hydrochloride
Hydroxypropyl-β-cyclodextrin
Caco-2 cell
Mathematical model

ABSTRACT

Chitosan nanoparticles (CS-NPs) have been used to enhance the permeability of furosemide and ranitidine hydrochloride (ranitidine HCl) which were selected as candidates for two different biopharmaceutical drug classes having low permeability across Caco-2 cell monolayers. Drugs loaded CS-NPs were prepared by ionic gelation of CS and pentasodium tripolyphosphate (TPP) which added to the drugs inclusion complexes with hydroxypropyl-β-cyclodextrin (HP-βCD). The stability constants for furosemide/HP-βCD and ranitidine HCl/HP-βCD were calculated as 335 M^{-1} and 410 M^{-1}, whereas the association efficiencies (AE%) of the drugs/HP-βCD inclusion complexes with CS-NPs were determined to be 23.0 and 19.5%, respectively. Zetasizer and scanning electron microscopy (SEM) were used to characterise drugs/HP-βCD-NPs size and morphology. Transport of both nano and non-nano formulations of drugs/HP-βCD complexes across a Caco-2 cell monolayer was assessed and fitted to mathematical models. Furosemide/HP-βCD-NPs demonstrated transport kinetics best suited for the Higuchi model, whereas other drug formulations demonstrated power law transportation behaviour. Permeability experiments revealed that furosemide/HP-βCD and ranitidine HCl/HP-βCD nano formulations greatly induce the opening of tight junctions and enhance drug transition through Caco-2 monolayers.

1. Introduction

Chitosan (CS), a partial deacetylation product of chitin that consists of glucosamine and N-acetylglucosamine, is a biocompatible, biodegradable, safe and low toxic polymer, particularly in the case of oral route of drug administration, with low immunogenicity possesses various applications in medical and pharmaceutical fields (Singla and Chawla, 2001; López-León et al., 2004; Wu et al., 2005). This polymer is widely used as a carrier for low molecular weight drugs, vaccines and DNA (Bowman and Leong, 2006). Nanoparticle (NP) formulations as excitement approaches to enhance the solubility and cellular permeability of drugs which result in improved clinical efficacy have been widely investigated in recent years (Xua et al., 2006; Li et al., 2009).

Statistics show that nearly 40% of the manufactured drugs through the world have unfavourable water solubility which limits the application of these medicines in physiological environments (Gao et al., 2008). Hydroxypropyl-β-cyclodextrin (HP-βCD) belongs to a large family of cyclic oligosaccharides which have been extensively studied are used to increase aqueous solubility and permeability of poorly soluble drugs (Loftsson and Brewster, 1996; Zhang et al., 2008).

Intracellular and paracellular pathways which believed as the most important pathways for drug absorption and permeation across cellular routes could be activated by CS-NPs which have a great potential to increasing the permeability of hydrophobic drugs (Huang et al., 2002; Dong et al., 2006; Gao et al., 2008; Sadeghi et al., 2008; Trapani et al., 2009). Paracellular drug transport is enhanced by CS-NPs transient and reversibly (Artursson et al., 1994) due to electrostatic interactions between positive charge of CS and negative charge of sialic acid involved in the cell tight junctions (Dodane et al., 1999; Lee et al., 2006; Wang et al., 2008). Depolymerisation of cellular F-actin as a consequence of the interactions between CS and ZO-1 (zonula occludin), a protein located in the cellular membrane, considered as another mechanism for raising drugs paracellular permeation using CS-NPs (Huang et al., 2002).

* Corresponding author. Tel.: +98 21 88009440; fax: +98 21 88009440.
E-mail address: Dorkoosh@tums.ac.ir (F.A. Dorkoosh).

0378-5173/$ – see front matter © 2011 Elsevier B.V. All rights reserved.
doi:10.1016/j.ijpharm.2011.11.016

Ranitidine hydrochloride (ranitidine HCl) ($C_{13}H_{22}N_4OS_3$ HCl, Mw = 350.9, pK_a = 0.2 for ionised form and 1.2 for unionised form), which has high solubility and low permeability, is a class III compound (Mirmehrabi et al., 2004) and furosemide ($C_{12}H_{11}ClN_2O_5S$, Mw = 330.7, pK_a = 4), with low solubility and permeability, is a class IV substance according to the biopharmaceutical classification system (Beyers et al., 2000).

The human colorectal adenocarcinoma cell line Caco-2, is used as a standard model to assessing drugs absorption and transportation (Zuo et al., 2000).

Raising the solubility and permeability of drugs using a cosolvent like (HP-βCD), decreasing the size of formulations and enhancing their permeation by CS-NPs as a polymeric drug carrier have been investigated in this research. Main approach in this research was assessing only the effects of CS-NPs as a nanoparticulate drug carrier in order to increasing drugs permeability. So, high soluble ranitidine HCl was also complexed with HP-βCD to ignore the permeation enhancing effects of CD. On the other hand, presenting logic mathematical models to describe and distinguish between nano and non-nano drug/HP-βCD formulations and determine the effects of CS-NPs in the transport of two drug formulations across the biological monolayer were investigated.

2. Materials and methods

2.1. Materials

ChitoClear® CS base (viscosity 1%, w/v solution, 463 mPa s and 95% degree of deacetylation) was purchased from Primex (Siglufjörður, Iceland). Caco-2 cells were obtained from the Institute Pasteur (Iran). Ranitidine HCl was received as a generous gift from Shahre Daru Pharmaceutical Company (Tehran, Iran), and furosemide was a generous gift from Chemidarou Pharmaceutical Company (Tehran, Iran). Pentasodium tripolyphosphate (TPP) was obtained from Merck (Darmstadt, Germany). HP-βCD was purchased from Sigma–Aldrich (Saint Louise, USA). HPLC- (high performance liquid chromatography) grade acetonitrile was acquired from Merck. All other reagents used in this study were of analytical grade.

2.2. HPLC analysis

Furosemide and ranitidine HCl analyses were performed by a fully automated HPLC (Knauer, Germany) containing a UV detector. A LiChrospher 100 RP8 EC (250 mm × 4.6 mm, 5-μm particle size) stainless steel analytical column was used for both drugs. When measuring the levels of furosemide, the mobile phase consisted of water and acetonitrile in a ratio of 60:40 (v/v). The mobile phase pH was adjusted to 3.5 by adding 25 μl of orthophosphoric acid to 100 ml water. The flow rate was 2 ml/min, and UV detection was achieved at 228 nm. When assessing ranitidine HCl levels, the mobile phase was prepared by phosphate buffer (10 mM, pH = 7.1) and acetonitrile in a ratio of 80:20 (v/v). The flow rate was 1 ml/min, and UV detection was achieved at 230 nm. Furosemide and ranitidine HCl were detected at retention times of 5.5 and 11 min, respectively.

2.3. Phase solubility studies of drugs/HP-βCD inclusion complexes

Stability and phase solubility analyses for the HP-βCD inclusion complexes of furosemide and ranitidine HCl were performed according to the method depicted by Higuchi and Connors (1965). Briefly, excess amounts of drugs were added to different concentrations of HP-βCD (1–5 mM) in 0.02 N HCl solutions. Light exposure was avoided, and the mixtures were rotated end-over-end for 72 h at 25 °C. After achieving equilibrium, excess amounts of drugs were filtered through a cellulose nitrate Sartorius filter (0.45 μm). The filtered solutions were then diluted with methanol and analysed by HPLC-UV at 228 and 230 nm for furosemide/HP-βCD and ranitidine HCl/HP-βCD, respectively. Analyses were used to determine the amounts of soluble drugs in the presence of different concentrations of HP-βCD, which functioned as a cosolvent and stabilizer. The $K_{1:1}$ stability constant (K_C) for both drugs was calculated from an initial straight line portion of the phase solubility diagram using the following equation:

$$K_C = \frac{\text{Slope}}{S_0 \times (1 - \text{Slope})} \quad (1)$$

In this equation, S_0 and Slope represent the intrinsic solubility of the drug and the Slope of the phase solubility diagram, respectively.

2.4. CS-NPs synthesis

CS-NPs were produced by ionic gelation method first described by Calvo et al. (1997). Electrostatic forces between negative species generated from the dissociation of TPP in aqueous solution and positively charged CS result in the formation of CS-NPs. In the present work, the molar ratio of CS/TPP was changed to achieve CS-NPs with optimal physicochemical properties. The hydrodynamic size, polydispersity index (PDI) and zeta potential of CS-NPs were evaluated in order to select the optimal CS/TPP molar ratio for nanoparticle formation.

To produce the NPs, CS was dissolved in acetic acid at concentrations of 0.75, 1.5, 2.25, 3, 3.75, and 4.5 mg/ml to form a positive charge on the ammonium groups of CS, allowing for suitable water solubility. In all cases, NPs were prepared by adding 8 ml of TPP solution (0.5 mg/ml) and 1 ml of the drug inclusion complexes (drugs + 5 mM HP-βCD) to 20 ml of CS solution (pH 4.5) with various concentrations (0.5, 1, 1.5, 2, 2.5, and 3 mg/ml) under stirring conditions at room temperature. NPs were obtained after ultracentrifugation at 20,000 × *g* for 1 h. To separate NPs from the solution, the supernatant was discarded, and the pellet was resuspended with deionised water. Finally, the produced NPs were characterised by Zetasizer 3000 HS (Malvern instrument, Malvern, Worcestershire, UK) at 25 °C with a detection angle of 90° to perform NPs size, zeta potential and PDI. Scanning electron microscopy (SEM) images of the synthesized NPs were taken by a ZIESS DSM 960A, SEM (Carl Zeiss Inc., Oberkochen, Germany).

2.5. Association efficiency, loading capacity, and drugs release profiles

To determine association efficiency (AE%) and loading capacity (LC%)of the drugs nano formulations, NP solutions were first ultracentrifuged (20,000 × *g* at 4 °C) for 1 h, then the supernatants were discarded and pellets resuspended by deionised water. The amounts of non-associated and -loaded drugs in supernatants were calculated by measuring the difference between total amounts of drugs added to the NPs solution and the quantity of unbounded drugs using HPLC methods according to the following equations:

$$\text{AE\%} = \frac{\text{total amounts of drugs} - \text{amounts of free drugs}}{\text{total amounts of drugs}} \times 100 \quad (2)$$

$$\text{LC\%} = \frac{\text{total amounts of drugs} - \text{amounts of free drugs}}{\text{NPs weight}} \times 100 \quad (3)$$

To obtain drugs release profiles, 1 mg of each lyophilised drugs were dissolved in 1 ml of 0.1 M phosphate buffered saline solution (PBS) at pH of 7.4 and 4.0, representing the physiological environment (Apical side) and endolysosomal compartment (Intracellular space), respectively. 1 ml of the both drugs/HP-βCD-NPs were incubated in a dialysis bag and immersed in 19 ml of PBS (Boonsongrit

et al., 2006). The glass containers of PBS buffer (pH 4.0 and 7.4) which were used to test the release profiles of drugs from CS-NPs were kept at 37 °C and stirred for 4 h. At 30, 60, 90, 150, and 240 min time intervals, 1 ml of the samples were withdrawn from the buffer medium and replaced with 1 ml of fresh medium. Released drug levels were detected using the previously mentioned HPLC methods. The percentage of the released drugs was calculated using the following equation:

$$\text{Release}(\%) = \left(\frac{\text{Released drug}}{\text{Total drug}}\right) \times 100$$

2.6. Release and transport kinetic studies

To analyse drugs release from CS-NPs and the transport mechanisms involved in crossing the Caco-2 monolayer, several different kinetic models were used to describe the optimal release and transport kinetics for ranitidine HCl/HP-βCD and furosemide/HP-βCD in both nano and non-nano formulations. Eq. (3) is based on the zero-order kinetics, indicative of uniform drug release from the matrix with respect to the time (Mansour et al., 2010) used to describe systems where the rates of drug release and transport are independent of drug concentration in the matrix (Shoaib et al., 2006; Amgaokar et al., 2011). It is represented by the following equation:

$$\frac{M_t}{M_\infty} = K_0 t, \tag{4}$$

where M_t/M_∞ is the fractional drug release, K_0 is the zero-order kinetic constant and t is time. First order kinetic describes systems for which the rate of drug release is dependent on the drug concentration (Amgaokar et al., 2011). First order kinetics is represented as:

$$\frac{M_t}{M_\infty} = 1 - \exp(-K_1 t), \tag{5}$$

where K_1 is the first order kinetic constant that is fitted according to the experimental data.

Eq. (6) is based on the Hixson–Crowell cube root model, which states that the mechanism of drug release depends upon the change in surface area or particle size (Hixson and Crowell, 1931). This model is represented as:

$$M_0^{1/3} - M_t^{1/3} = K_{HC} t, \tag{6}$$

where M_0 is the initial amount of drug in the carrier, M_t is the amount of drug released at time t, and K_{HC} is a kinetic constant.

The Higuchi model (1963) describes drug release from a matrix as a diffusion process based on Fick's law which represented as the square root of a time-dependent process (Siepmanna and Peppas, 2000). The equation for the Higuchi model is as follows:

$$\frac{M_t}{M_\infty} = K_H t^{1/2}, \tag{7}$$

where M_t/M_∞ is the fractional drug release, and K_H is the Higuchi constant.

Finally, Eq. (8), derived by Korsmeyer–Peppas (1983), represents power law release kinetics which follows non-Fickian release mechanism used to describe drug release that has an exponential relationship with respect to time. This model is represented by the following equation:

$$\frac{M_t}{M_\infty} = K_P t^n, \tag{8}$$

where n, like other constants in the above models, was determined by fitting release and transport data with respective models, and K_P represents the power law constant. Both of the dedicated parameters are experimentally determined factors and depend on the geometry of carrier boundaries. All practically achieved data were fitted by Maple™ 14 to evaluate theoretical models of drug release and transport.

Sum square of errors (SSE), sum square of regression (SSR) and sum square of total variation (SST) using Eqs. (9), (10), and (11), respectively, were calculated to evaluate the coefficients of determination (R^2) for each model and the accuracy of the best fitted data by the suggested mathematical models based on Eq. (12). These equations are as follows:

$$\text{SSE} = \sum_{i=1}^{n} e^2 = \sum_{i=1}^{n} (y_i - yf_i)^2, \tag{9}$$

$$\text{SST} = \sum_{i=1}^{n} (y_i - \bar{y})^2, \tag{10}$$

$$\text{SSR} = \text{SST} - \text{SSE}, \tag{11}$$

$$R^2 = 1 - \frac{\text{SSE}}{\text{SST}}, \tag{12}$$

where y_i represents the vector of dependent observed variables for an observation, yf_i is a fitted variable value, e is the error vector and $\bar{y}$ is the mean value of y_i.

The relative sizes of the sums of squares terms demonstrate how "good" the regression is in terms of fitting the calibration data. If the regression is "perfect", then SSE is zero, and R^2 will be 1.

2.7. Caco-2 cell culture and preparation of the cell monolayer

Caco-2 cells (passage number 40–45) were maintained at 37 °C and grown in 25 ml Nunc flasks in an incubator with a controlled, humidified atmosphere consisting of 5% CO_2 and 95% air. Cells were cultured in an enriched medium consisting of RPMI-1640, Dulbecco's modified Eagle medium (DMEM), fetal bovine serum (FBS) and penicillin/streptomycin (100 U/ml) in a ratio of 50:35:15:1 which was changed every second day. Cells were trypsinised by trypsin–EDTA (1%) and resuspended in a culture medium at 70–80% confluency.

Cells were seeded on semipermeable filter inserts (Nunc 24-well Transwell plates) at 4×10^5 cells/cm^2 density on 0.47-cm^2 polycarbonate membranes with a pore size of 0.4 μm (Markowska et al., 2001). Caco-2 cell monolayers were used after 21 days of incubation on the filter inserts. To enhance cell adhesion, filters were precoated prior to seeding the cells with 40 μl of diluted rat tail collagen (type I) solution in 1 N acetic acid in a ratio of 1:9 (10× dilution) (Masungi et al., 2004). Coated filter inserts were dried in an incubator overnight, and cells were then seeded on the polycarbonate filters.

2.8. Transport studies

All transport experiments were conducted at 37 °C under laminar air flow. Prior to the transport experiments, cells were washed twice with PBS and preincubated with Hanks' balanced salt solution (HBSS, pH 7.4) supplemented with 25 mM HEPES for 25 min. Culture medium was replaced by transition buffer (HBSS–HEPES) during the transportation experiments. Drugs in both nano and non-nano formulations were added to the apical compartment of the monolayer at a final concentration of 1 mg/ml in 0.5 ml HBSS–HEPES buffer. The basolateral side of the monolayer contained only 1 ml of transition buffer. All transport analyses were conducted in the apical (A) to basolateral (B) direction of the monolayer. At the defined time intervals (30, 60, 90, 150 and 240 min), 200 μl of samples were removed from the basolateral side of the monolayer and replaced with an equal amount of fresh transition buffer. The collected samples were analysed using the previously mentioned HPLC methods for each drug.

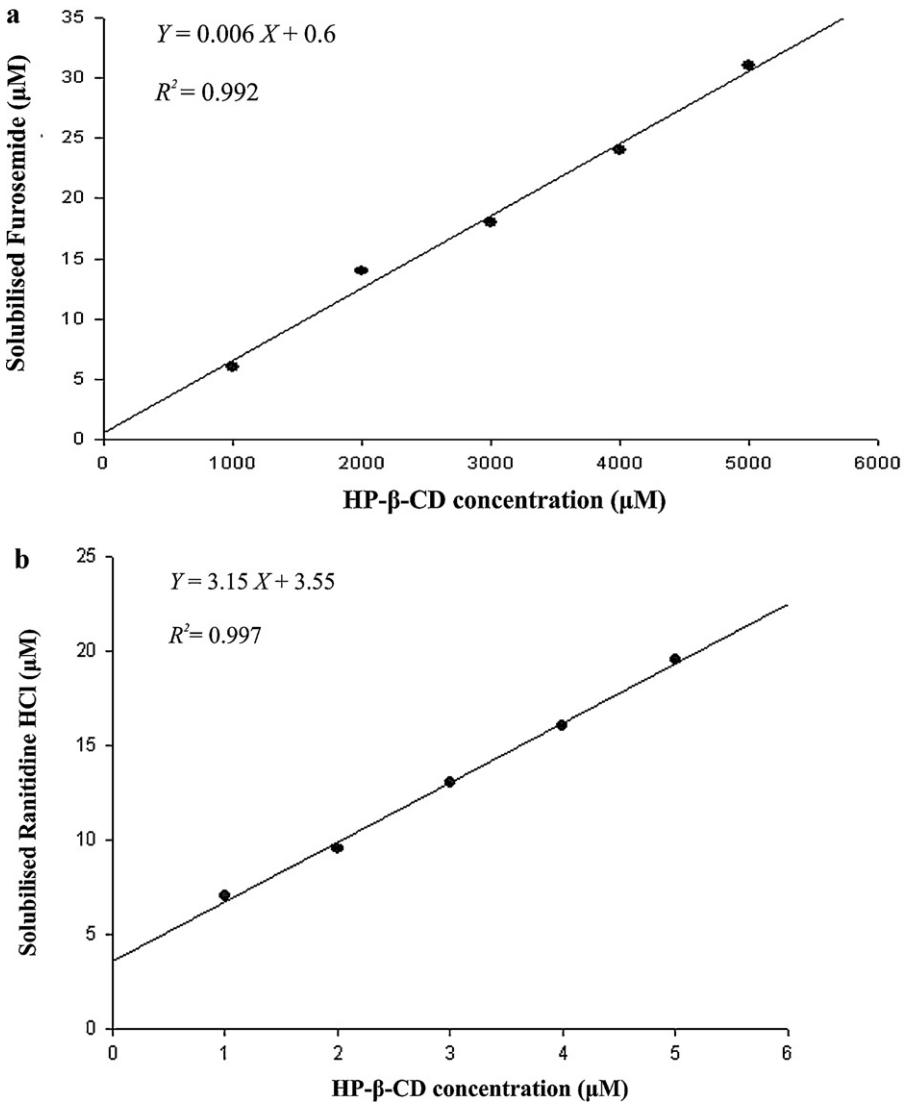

Fig. 1. Phase solubility diagrams of (a) furosemide/HP-βCD and (b) ranitidine HCl/HP-βCD in the presence of different concentrations of HP-βCD in a 0.02 N solution of HCl incubated at 35 ± 2 °C.

Apparent permeability coefficients (P_{app}) for each formulation were calculated according to the following equation:

$$P_{app} = \frac{V_r \times C_r}{A \times t \times C_0}, \quad (13)$$

where V_r corresponds to the volume of the receptor compartment, C_r is the drug concentration at the receiver compartment, A represents the filter surface area, t is time and C_0 represents the initial drug concentration at the apical side.

2.9. Transepithelial electrical resistance measurement (TEER assay)

Transepithelial electrical resistance (TEER) of Caco-2 cell monolayers was measured 15–21 days after seeding cells on the filter inserts. An EVOM equipped with "chopstick" electrodes (World Precision Instruments, Sarasota, FL) was used to ensure the integrity of Caco-2 cell monolayers on the filter inserts. TEER measurements were also performed during the permeation experiment at predetermined time intervals (0, 2, 4, 8, 12 and 24 h) to assess the effects of CS-NPs on the opening of tight junction barriers during and after the transport experiment. TEER values were calculated based on the following equation:

$$\text{TEER} = (R_{\text{monolayer}} - R_{\text{blank}}) \times A(\Omega\,\text{cm}^2),$$

where $R_{\text{monolayer}}$ is the measured resistance of Caco-2 monolayer, R_{blank} represents the resistance of filter inserts without cell monolayer, and A is the available filter inserts surface area.

2.10. Statistical analysis

Data are reported as mean ± standard deviation from 3 independent experiments. Statistical significance between mean values was calculated using independent sample t-test and one-way analysis of variance (ANOVA) with Dunnett's T3 post hoc test (SPSS 15.0, SPSS, Inc.). Probability values <0.05 were considered significant.

3. Results and discussion

3.1. Phase solubility results

Phase solubility of furosemide and ranitidine HCl with HP-βCD was assayed in a solution of 0.02 N HCl at 35 ± 2 °C. According to

Table 1
Characterisation of CS-NPs using various CS/TPP molar ratios.

CS/TPP molar ratio	Particle size (nm) ± *SD*	Zeta potential (mV) ± *SD*	PDI ± *SD*
1:1	815 ± 20	+23 ± 7.52	0.58 ± 0.24
2:1	243 ± 15	+35 ± 4.50	0.38 ± 0.42
3:1	391 ± 35	+32 ± 3.51	0.68 ± 0.31
4:1	196 ± 22	+41 ± 6.53	0.33 ± 0.18
5:1	230 ± 16	+36 ± 7.46	0.40 ± 0.28
6:1	1062 ± 45	+22 ± 5.50	0.47 ± 0.34

Fig. 1a and b, increasing HP-βCD concentrations resulted in a linear enhancement in the solubility of furosemide and ranitidine HCl. These diagrams depicted a linear relationship between the amounts of solubilised drug in 0.02 N HCl and the concentration of HP-βCD over an indicated range (Mora et al., 2010). The provided diagrams can be classified as A_L-type solubility diagrams, according to the Higuchi and Connors method. These diagrams indicate the formation of a first order dependency of the interactions on the cyclodextrin concentration (Loftsson and Brewster, 1996). Using the stability constant, Eq. (1) which mentioned previously, stability constants (K_C) for furosemide/HP-βCD and ranitidine HCl/HP-βCD were determined to be 335 M^{-1} and 410 M^{-1}, respectively. Based on these results, it can be concluded that stable inclusion complexes between HP-βCD and drug in a 1:1 molar ratio have been formed (Onyeji et al., 2009).

3.2. Nanoparticle characterisation

Measured size, PDI, and zeta potential of CS-NPs made with different CS/TPP molar ratios have been provided in Table 1. A CS/TPP molar ratio of 4:1 demonstrated superior physicochemical properties, such as low particle size, low PDI and high zeta potential, which represents desirable colloidal stability relative to the other nanoparticle formulations (Mohanraj and Chen, 2006), was selected for loading both drugs (Table 2). At 1:1 CS/TPP molar ratio, the equal amounts of CS positive charge and TPP negative charge results in the formation of agglomerate particles where by increasing CS concentration from 0.5 mg/ml to 2 mg/ml, long amine groups prevent the TPP anions adsorption and probably, results in a high amount of positive electrical double layer thickness which prevents particles aggregation. Raising CS concentration more than 2 mg/ml results in the formation of huge amounts of CS positive species, which prevents the desirable interaction between positive and negative charges to produce CS-NPs. Optimum zeta potential and PDI for the CS-NPs, were achieved by increasing the CS/TPP concentration ratio to 4:1. Increasing the CS/TPP molar ratio to more than 4:1 resulted in reduced zeta potential and increased PDI. AE% and LC% for the produced ranitidine HCl/HP-βCD-NPs were calculated as 23% and 18% whereas these parameters were 19.5% and 14% in the case of furosemide/HP-βCD-NPs. The SEM images of the free-form CS-NPs (Fig. 2a) as well as furosemide/HP-βCD- and ranitidine HCl/HP-βCD-loaded CS-NPs (Fig. 2b and c) are provided. Particles without associated drug have a smooth spherical shape, whereas drug-loaded NPs have an asymmetric, rough spherical morphology, probably due to the drugs attachment.

3.3. In vitro drug release studies

3.3.1. Experimental drug release studies

Ranitidine HCl/HP-βCD- and furosemide/HP-βCD-loaded CS-NPs were immersed in PBS (pH 7.4 and 4.0) to simulate the physiological pH observed at the apical side and endolysosomal compartment of Caco-2 cells, respectively. As depicted in Fig. 3a and b, ranitidine HCl/HP-βCD and furosemide/HP-βCD have differing release profiles because of their different chemical structures.

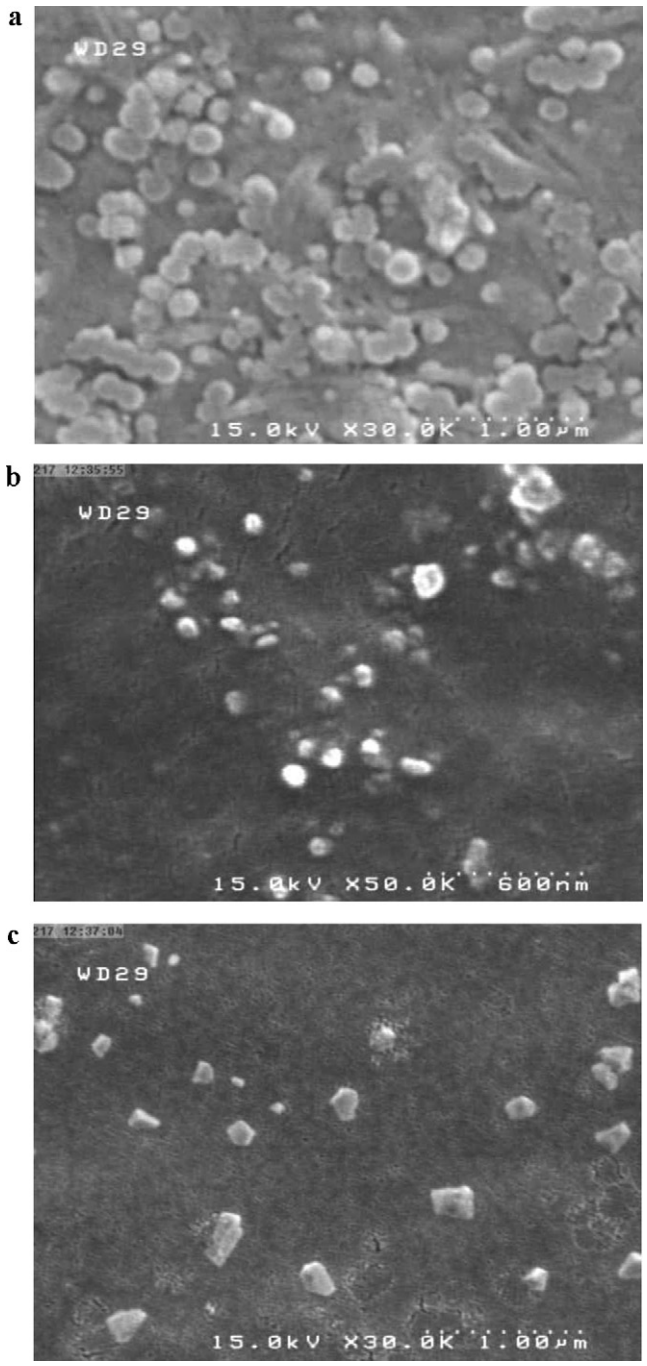

Fig. 2. SEM images of (a) hallow CS-NPs, (b) furosemide/HP-βCD-CS-NPs and (c) ranitidine HCl/HP-βCD-CS-NPs.

Faster release kinetic was observed for ranitidine HCl/HP-βCD at the lower pH (4.0) compared to its release at the neutral pH. The amine groups presented in the structure of ranitidine HCl/HP-βCD could protonate at the lower pH, and as a result, the drug would solubilise in water more easily and releases from the CS matrix to the aqueous environment. As illustrated in Fig. 3, 80% of ranitidine HCl/HP-βCD was released from CS-NPs at pH 4.0 after 90 min, whereas only 50% of ranitidine HCl/HP-βCD was released at pH 7.4. In contrast, furosemide/HP-βCD release from CS-NPs is slower relative to ranitidine HCl/HP-βCD during 4-h incubation at pH 4.0.

At acidic pH values, the protonated amine groups electrostatically repulsed by CS positive charge, and release occurred faster than ranitidine release at neutral pH. The burst effect followed by

Table 2
Characterisation of drugs loaded CS-NPs.

Drugs-NPs	Size (nm) ± *SD*	PDI ± *SD*	Zeta potential (mV) ± *SD*	AE%	LC%
Ranitidine HCl/HP-βCD-NPs	244.5 ± 24	0.40 ± 0.15	+35 ± 12	23.0	18.0
Furosemide/HP-βCD-NPs	196.0 ± 35	0.33 ± 0.22	+41 ± 16	19.5	14.0

Table 3
Release parameters for the nano formulation of ranitidine HCl/HP-βCD obtained after fitting data with five different mathematical models of drug release kinetics.

pH	Fitted theoretical models									
	Zero order		First order		Hixson–Crowell		Higuchi		Power law[a]	
pH 4.0	K_0	0.40	K_1	0.01	K_{HC}	0.01	K_H	0.76	K_P	765.30
	R^2	0.63	R^2	0.51	R^2	0.75	R^2	0.74	R^2	0.84
									n	0.05
									SSE	1045.26
									SST	6450.18
									SSR	5404.92
pH 7.4	K_0	0.27	K_1	0.01	K_{HC}	0.005	K_H	304.46	K_P	507.39
	R^2	0.71	R^2	0.54	R^2	0.81	R^2	0.80	R^2	0.89
									n	0.05
									SSE	309.59
									SST	2811.92
									SSR	2502.32

[a] Significant data.

sustained release was observed for ranitidine HCl/HP-βCD release from CS-NPs. Miro et al. (2006) have shown that, hydrophilic CDs (HP-βCD) could be able to prolong drug release, so it can be concluded that CS-NPs are responsible for the preliminary burst effect followed by sustained release.

At lower pH values (pH 4.0) in contrast to higher pH values (pH 7.4), the ability of carboxylic group of furosemide to be deprotonated decreases which results in decreasing the solubility of furosemide in aqueous medium at pH 4.0 compare to its solubility at neutral pH. Furosemide/HP-βCD release showed sustained release profile at acidic pH compare to its release at neutral pH (Fig. 3b).

3.3.2. Theoretical drug release studies

To determine the best equation to describe drugs release profiles for different physiological situations, all experimental release data were fitted by five mathematical models. Results for fitting ranitidine HCl/HP-βCD and furosemide/HP-βCD release profiles into respective equations are provided in Tables 3 and 4, respectively. Fitting release data with the five different equations revealed that the ranitidine HCl/HP-βCD release profile was more appropriate for the power law model, with correlation coefficients of 0.84 and 0.89 for pH 4.0 and 7.4, respectively (Fig. 4a). This finding suggests that the relationship between the concentration of released drug versus time is exponential and concentration independent. The power law release exponent (n), which is indicative of a drug release mechanism, fit similar to other equation constants when plotting the experimental data. The furosemide/HP-βCD release profile was best fit to the zero order kinetic model, with correlation coefficients of 0.95 for both pH values which shows a non-Fickian (case II transport) release behaviour (Fig. 4b). A linear relationship between the concentrations of the released drug versus time indicates a concentration independent profile for furosemide/HP-βCD release from CS-NPs.

3.4. Monolayer integrity

The development of Caco-2 cell monolayers on polycarbonate filter inserts was investigated by TEER for 21 days. The measured TEER value for Caco-2 cells grown on filters after noted time was 600 Ω cm^2, which indicates the formation of tight junctions and good cell integrity. The addition of drugs in the forms of HP-βCD/drugs-NPs and drugs/HP-βCD formulations resulted in the reduced TEER values (Fig. 5). Nano formulations caused more considerable reduction in the cell integrity relative to non-nano formulations particularly in the case of furosemide/HP-βCD-NPs. The decrease in cell integrity which was observed in the presence of drugs/HP-βCD formulations less than HP-βCD/drugs-NPs, suggested slight permeation enhancement of HP-βCD due to its effects on the monolayer TEER value which was similarly reported by Zuo

Table 4
Release parameters for the nano formulation of furosemide/HP-βCD obtained after fitting data with five different mathematical models of drug release kinetics.

pH	Fitted theoretical models									
	Zero order[a]		First order		Hixson–Crowell		Higuchi		Power law	
pH 4.0	K_0	0.21	K_1	0.01	K_{HC}	0.004	K_H	4.60	K_P	0.38
	R^2	0.95	R^2	0.69	R^2	0.93	R^2	0.92	R^2	0.94
	SSE	70.81							n	0.90
	SST	1299								
	SSR	1228								
pH 7.4	K_0	0.45	K_1	0.01	K_{HC}	0.013	K_H	4.60	K_P	0.38
	R^2	0.95	R^2	0.69	R^2	0.81	R^2	0.92	R^2	0.94
	SSE	253.40							n	0.90
	SST	5613.30								
	SSR	5359.60								

[a] Significant data.

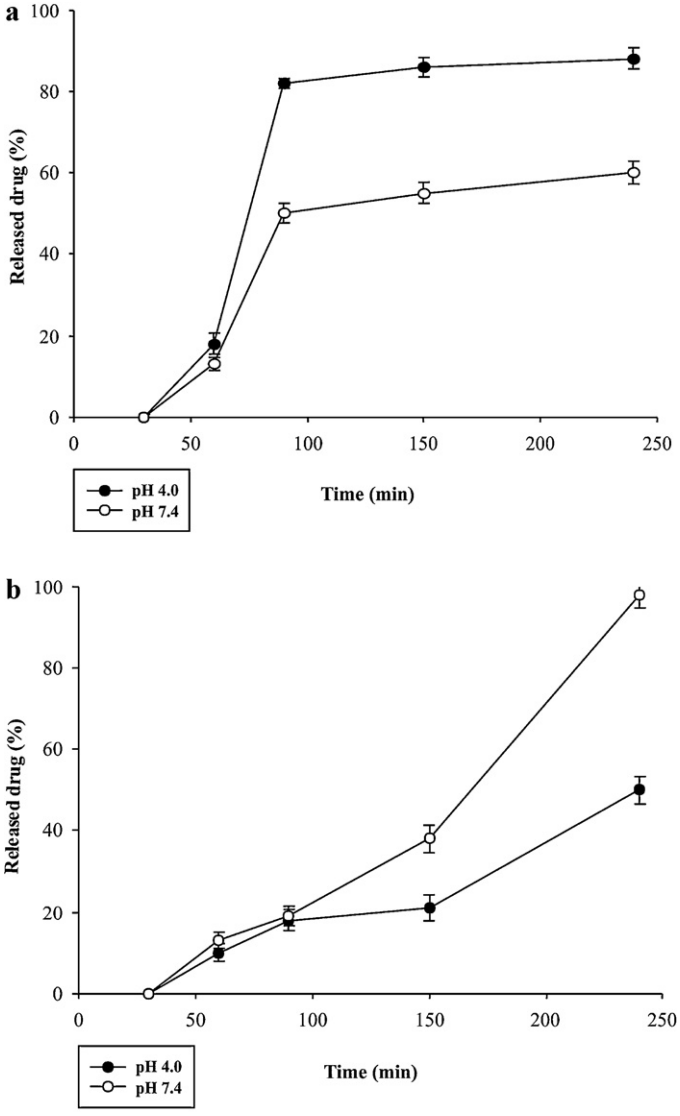

Fig. 3. In vitro release of (a) ranitidine HCl/HP-βCD and (b) furosemide/HP-βCD from CS-NPs in 0.1 M PBS buffer at pH 7.4 (○) and pH 4.0 (●). Data are shown as mean ± *SD* (*n* = 3).

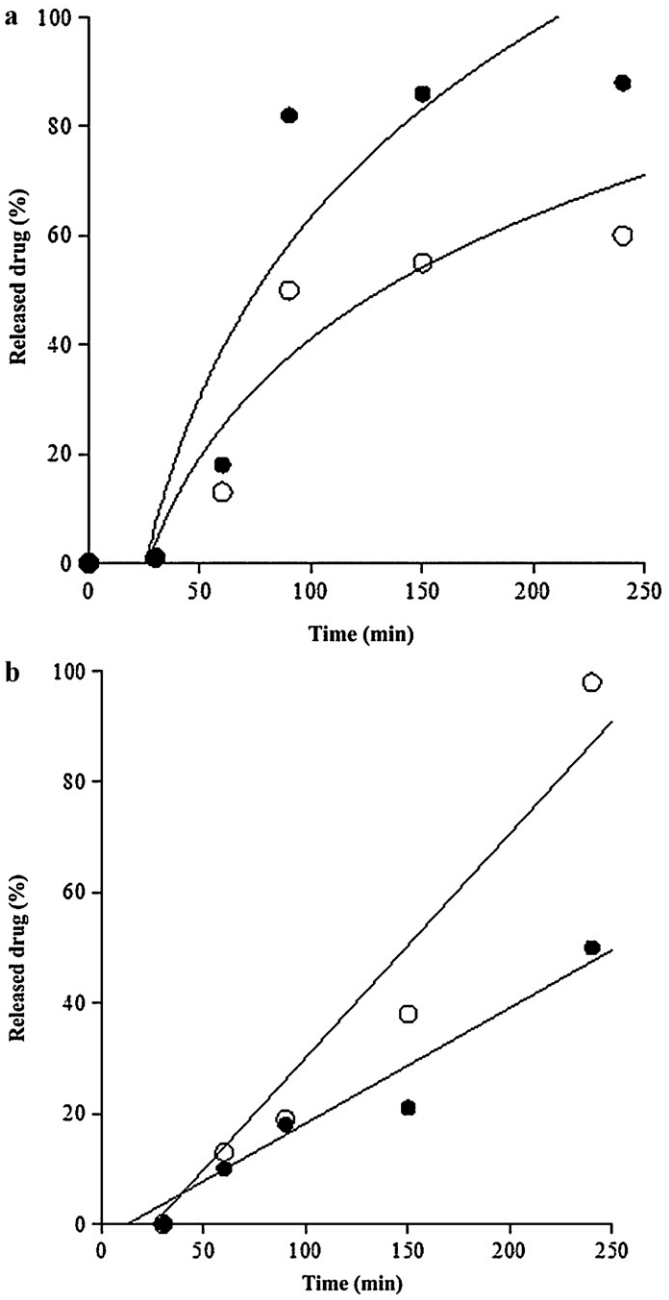

Fig. 4. Model fit of the experimentally determined amounts of (a) ranitidine HCl/HP-βCD and (b) furosmide/HP-βCD release from CS-NPs at pH 4.0 (●) and pH 7.4 (○). Experimental and theoretical data are represented by circles and black solid lines, respectively.

et al. (2000). The furosemide/HP-βCD nano formulation resulted in lower TEER values than all other formulations. Probably, higher zeta potential of furosemide/HP-βCD-NPs is an acceptable reason for the observed phenomenon.

3.5. Drug transport

Both nano and non-nano formulations of drugs were added to the apical side of the Caco-2 cell monolayer to evaluate the effects of CS-NPs on the opening of cell tight junctions. Apparent permeability for each formulation is provided in Table 5. A significant difference was not detected between the transports of the ranitidine HCl/HP-βCD and ranitidine HCl/HP-βCD-NPs, when comparing with the corresponding formulations of furosemide (Fig. 6). Equations and correlation coefficients for nano and non-nano formulations of ranitidine HCl/HP-βCD and furosemide/HP-βCD are provided in Tables 6 and 7 were applied to the five previously mentioned equations, respectively. Slow transport kinetics for both ranitidine HCl/HP-βCD formulations was best fitted by the power law models (Fig. 7a). Furosemide/HP-βCD transport across the monolayer was best fitted by the power law equation, whereas furosemide/HP-βCD-NPs transport was more appropriate for the Higuchi kinetic model (Fig. 7b). Faster apical to basolateral transportation of nano furosemide/HP-βCD was observed due to its higher positive zeta potential and smaller particle size, compare to the nano ranitidine

Table 5
Permeability coefficients of ranitidine HCl/HP-βCD and furosemide/HP-βCD in both nano and non-nano formulations.

Drugs	P_{app} ($\times 10^{-6}$ cm/S) ± *SD*
Furosemide/HP-βCD-NPs	7.56 ± 0.21
Furosemide/HP-βCD	3.4 ± 0.24
Ranitidine HCl/HP-βCD-NPs	4.23 ± 0.56
Ranitidine HCl/HP-βCD	3.45 ± 0.12

Table 6
Transport of ranitidine HCl/HP-βCD in both nano and non-nano formulations across Caco-2 cell monolayer fitted by five theoretical models.

Drugs	Fitted theoretical models									
	Zero order		First order		Hixson–Crowell		Higuchi		Power law[a]	
Ranitidine HCl/HP-βCD	K_0	0.009	K_1	0.004	K_{HC}	0.0002	K_H	0.2	K_P	17.12
	R^2	0.69	R^2	0.6	R^2	0.71	R^2	0.81	R^2	0.91
									n	0.05
									SSE	0.26
									SST	2.94
									SSR	2.68
Ranitidine HCl/HP-βCD-NPs	K_0	0.01	K_1	0.003	K_{HC}	0.0002	K_H	0.23	K_P	0.5
	R^2	0.86	R^2	0.76	R^2	0.77	R^2	0.94	R^2	0.99
									n	0.05
									SSE	0.02
									SST	3.82
									SSR	3.79

[a] Significant data.

Table 7
Transport of furosemide/HP-βCD in both nano and non-nano formulations across Caco-2 cell monolayers fitted by five theoretical models.

Drugs	Fitted theoretical models									
	Zero order		First order		Hixson–Crowell		Higuchi[a]		Power law[a]	
Furosemide/HP-βCD	K_0	0.01	K_1	0.009	K_{HC}	0.0003	K_H	0.35	K	28.23
	R^2	0.81	R^2	0.69	R^2	0.84	R^2	0.90	R^2	0.97
									n	0.05
									SSE	0.23
									SST	9.45
									SSR	9.21
Furosemide/HP-βCD-NPs	K_0	0.02	K_1	0.003	K_{HC}	0.0005	K_H	0.5	K	0.28
	R^2	0.97	R^2	0.93	R^2	0.81	R^2	0.99	R^2	0.97
							SSE	0.10	n	0.05
							SST	19.68		
							SSR	19.58		

[a] Significant data.

HCl/HP-βCD formulation. Probably, higher zeta potential enabled furosemide/HP-βCD-NPs to interact stronger with the tight junctions which subsequently resulted in improved transition. In contrast to the difference observed between nano and non-nano

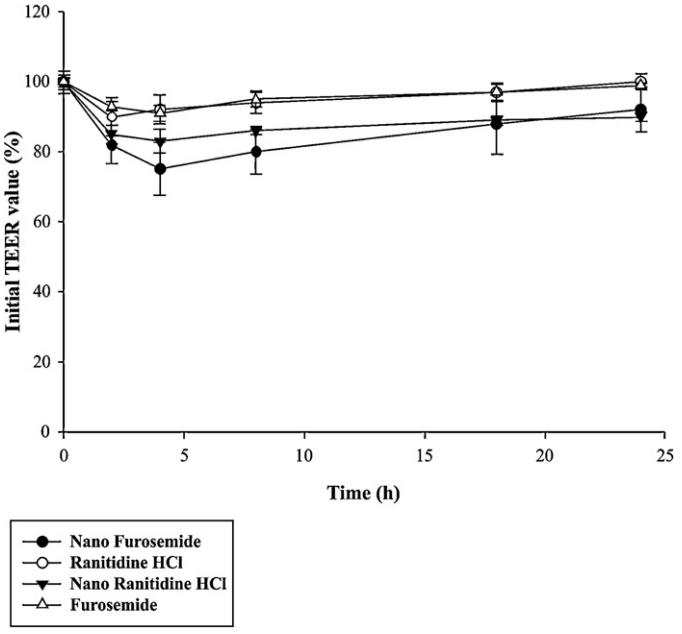

Fig. 5. Transepithelial electrical resistance (TEER) values of Caco-2 monolayers measured after the addition of ranitidine HCl/HP-βCD and furosemide/HP-βCD, in both nano and non-nano formulations, to the apical side of Caco-2 cell monolayers over a period of 24 h. Data are shown as mean ± *SD* (*n* = 3).

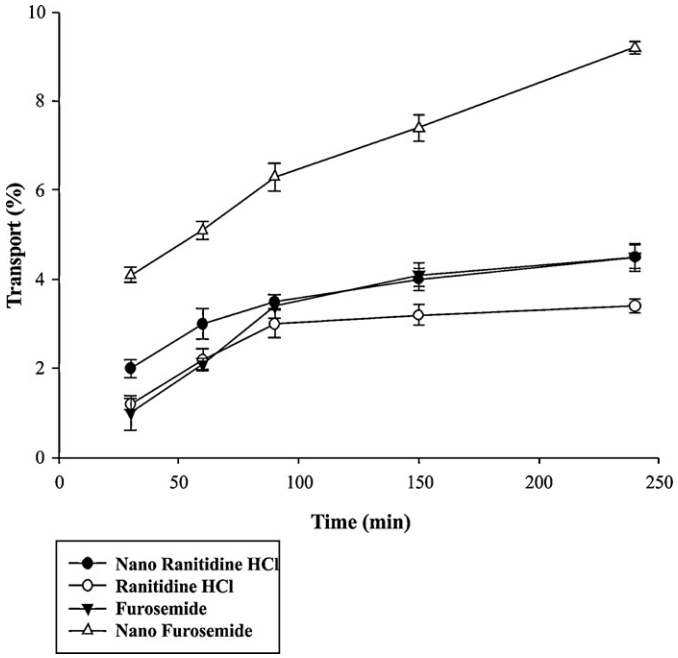

Fig. 6. Comparison of the apical to basolateral transport of ranitidine HCl/HP-βCD and furosemide/HP-βCD, in both nano and non-nano formulations, across Caco-2 cell monolayer. The amounts of drugs on the basolateral side were measured at the specified time intervals after the addition of drug formulation (1 mg/ml). The amounts of transported drugs are expressed as a percentage of the initial drugs concentration on the apical side. Data are shown as mean ± *SD* (*n* = 3).

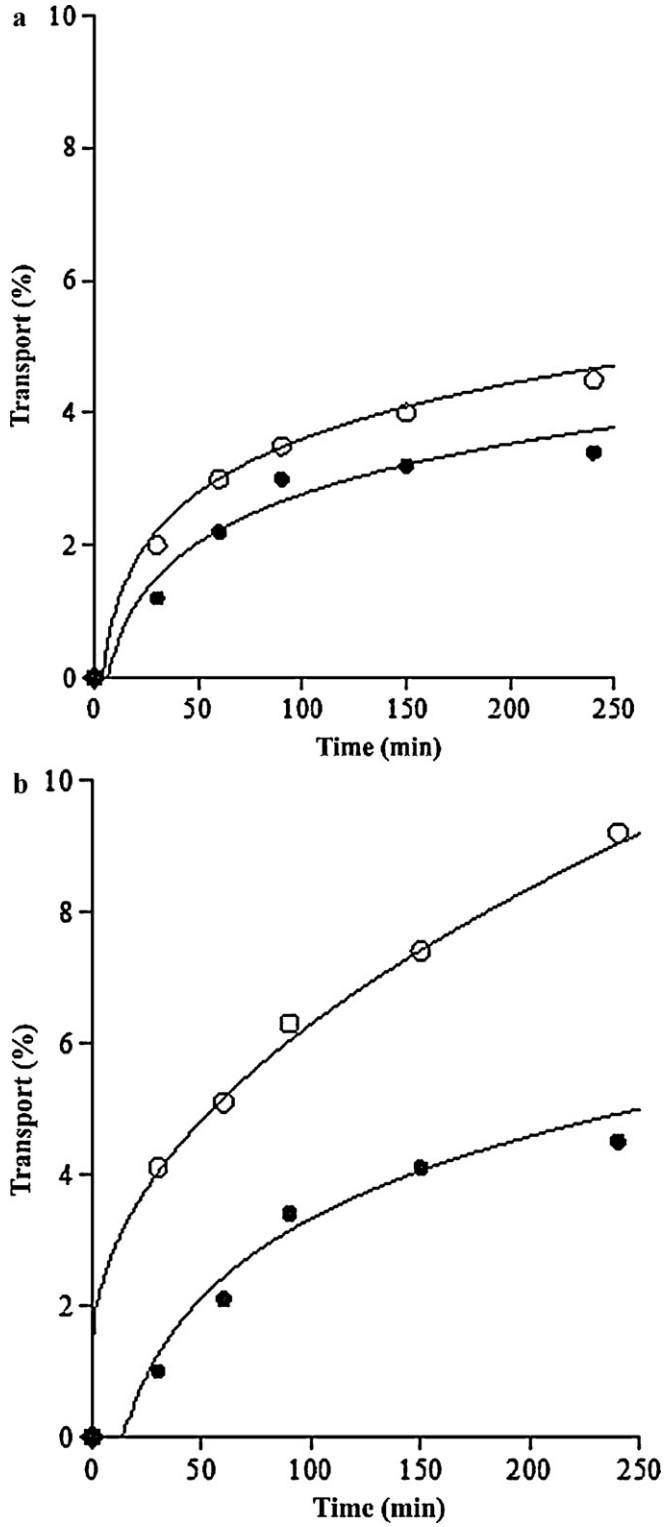

Fig. 7. Model fit of the experimentally determined amounts of drugs, in nano and non-nano formulations, transported across Caco-2 cell monolayers: (a) ranitidine HCl/HP-βCD-NPs (○) and ranitidine HCl/HP-βCD (●); (b) furosmid/HP-βCD-NPs (○) and furosmide/HP-βCD (●).

formulations of furosemide/HP-βCD, a significant difference between the transport of nano and non-nano ranitidine HCl/HP-βCD formulations across the biological monolayer was not detected. A probable reason to justify this phenomenon is the relatively larger nano ranitidine HCl/HP-βCD particle size and its lower positive zeta potential than that of the nano furosemide/HP-βCD formulation.

4. Conclusion

Ranitidine HCl and furosemide were complexed with HP-βCD to increase their water solubility and stability. This procedure enhanced the aqueous solubility of both drugs and increased drug permeability across the Caco-2 monolayer. Nano formulation of drugs with CS-NPs increased drug permeation across the cell monolayer by inducing electrostatic interactions with paracellular proteins, results in the opening of tight junctions. Furosemide/HP-βCD-NPs transportation across the cell monolayer showed fast transport kinetics best suited for the Higuchi mathematical model, whereas the kinetics of other drug formulations were better described by the power law model. Lower nano furosemide/HP-βCD particle size and higher zeta potential are the main reasons for this enhanced drug transport across the Caco-2 monolayer. The increased rate of transition across a biological membrane for the nano furosemide/HP-βCD formulation relative to the non-nano formulation in contrast to the similar transport rates for nano and non-nano ranitidine HCl/HP-βCD formulations suggests that particle size and zeta potential are critical factors for drug transport across the Caco-2 monolayer.

References

Amgaokar, Y.M., Chikhale, R.V., Lade, U.B., Biyani, D.M., Umekar, M.J., 2011. Design, formulation and evaluation of transdermal drug delivery system of budesonide. Dig. J. Nanomater. Bios. 6, 475–497.
Artursson, P., Lindmark, T., Davis, S.S., Illum, L., 1994. Effect of chitosan on the permeability of monolayer of intestinal epithelial cells (Caco-2). Pharm. Res. 11, 1358–1361.
Beyers, H., Malan, S.F., van der Watt, J.G., de Villiers, M.M., 2000. Structure–solubility relationship and thermal decomposition of furosemide. Drug Dev. Ind. Pharm. 26, 1077–1083.
Boonsongrit, Y., Mitrevej, A., Mueller, B.W., 2006. Chitosan drug binding by ionic interaction. Eur. J. Pharm. Biopharm. 62, 267–274.
Bowman, K., Leong, K.W., 2006. CS-NPs for oral drug and gene delivery. Int. J. Nanomed. 1, 117–128.
Calvo, P., Remunan-Lopez, C., Vila-Jato, J.L., Alonso, M.J., 1997. Novel hydrophilic chitosan–polyethylene oxide nanoparticles as protein carriers. J. Appl. Polym. Sci. 63, 125–132.
Dodane, V., Khan, M.A., Merwin, J.R., 1999. Effect of chitosan on epithelial permeability and structure. Int. J. Pharm. 182, 21–32.
Dong, W.Y., Maincent, P., Bodmeier, R., 2006. In vitro and in vivo evaluation of carbamazepine-loaded enteric microparticles. Int. J. Pharm. 331, 84–92.
Gao, L., Zhang, D., Chen, M., 2008. Drug nanocrystals for the formulation of poorly soluble drugs and its application as a potential drug delivery system. J. Nanopart. Res. 10, 845–862.
Higuchi, T., Connors, K.A., 1965. Phase-solubility techniques. Adv. Anal. Chem. Instrum. 4, 117–212.
Higuchi, T., 1963. Mechanism of sustained action medication. Theoretical analysis of rate of release of solid drugs dispersed in solid matrices. J. Pharm. Sci. 52, 1145–1149.
Hixson, A.W., Crowell, J.H., 1931. Dependence of reaction velocity upon surface and agitation (I) theoretical consideration. Ind. Eng. Chem. 23, 923–931.
Huang, M., Ma, Z., Khor, E., Lim, L.-Y., 2002. Uptake of FITC-CS-NPs by A549 cells. Pharm. Res., 19.
Korsmeyer, R.W., Gurny, R., Doelker, E., Buri, P., Peppas, N.A., 1983. Mechanism of solute release from porous hydrophilic polymers. Int. J. Pharm. 15, 25–35.
Lee, D-W., Shirley, S.A., Lockey, R.F., Mohapatra, S.S., 2006. Thiolated chitosan nanoparticles enhance anti-inflammatory effects of intranasally delivered theophylline. Respir. Res. 7, 112–121.
Li, F., Li, J., Wen, X., Zhou, S., Tong, X., Su, P., Li, H., Shi, D., 2009. Anti-tumor activity of paclitaxel-loaded CS-NPs: an in vitro study. Mater. Sci. Eng., doi:10.1016/j.msec.2009.07.001.
Loftsson, T., Brewster, M.E., 1996. Pharmaceutical applications of cyclodextrins. 1. Drug solubilization and stabilization. J. Pharm. Sci. 85, 1017–1025.
López-León, T., Carvalho, E.L.S., Seijo, B., Ortega-Vinuesa, J.L., Bastos-González, D., 2004. Physicochemical characterization of CS-NPs: electrokinetic and stability behavior. J. Colloid Interf. Sci. 283, 344–351.
Mansour, H.M., Sohn, M., Al-Ghananeem, A., DeLuca, P.P., 2010. Materials for pharmaceutical dosage forms: molecular pharmaceutics and controlled release drug delivery aspects. Int. J. Mol. Sci. 11, 3298–3322.
Markowska, M., Oberle, R., Juzwin, S., Hsu, C.-P., Gryszkiewicz, M., Streeter, A.J., 2001. Optimizing Caco-2 cell monolayers ti increase throughput in drug intestinal absorption analysis. J. Pharmacol. Toxicol. Methods 46, 51–55.

Masungi, C., Borremans, C., Willems, B., Mensch, J., Van Dijck, A., Augustijns, P., Brewster, E.M., Noppe, M., 2004. Usefulness of a novel Caco-2 cell perfusion system. I. In vitro prediction of the absorption potential of passively diffused compounds. J. Pharm. Sci., doi:10.1002/jps.20149.

Mirmehrabi, M., Rohani, S., Murthy, K.S.K., Radatus, B., 2004. Solubility, dissolution rate and phase transition studies of ranitidine hydrochloride tautomeric forms. Int. J. Pharm. 282, 73–85.

Miro, A., Quaglia, F., Giannini, L., Cappello, B., La Rotonda, M.I., 2006. Drug/cyclodextrin solid systems in the design of hydrophilic matrices: a strategy to modulate drug delivery rate. Curr. Drug Deliv. 3, 373–378.

Mohanraj, V.J., Chen, Y., 2006. Nanoparticles—a review. Trop. J. Pharm. Res. 5, 561–573.

Mora, M.J., Longhi, M.R., Granero, G.E., 2010. Synthesis and characterization of binary and ternary complexes of diclofenac with a methyl-β-CD and monoethanolamine and in vitro transdermal evaluation. Eur. J. Med. Chem. 45, 4079–4088.

Onyeji, C.O., Omoruyi, S.I., Oladimeji, F.A., Soyinka, J.O., 2009. Physicochemical characterization and dissolution properties of binary systems of pyrimethamine and 2-hydroxypropyl-β-cyclodextrin. Afr. J. Biotechnol. 8, 1651–1659.

Sadeghi, A.M.M., Dorkoosh, F.A., Avadi, M.R., Saadat, P., Rafiee-Tehrani, M., Junginger, H.E., 2008. Preparation, characterization and antibacterial activities of chitosan, N-trimethyl chitosan (TMC) and N-diethylmethyl chitosan (DEMC) nanoparticles loaded with insulin using both the ionotropic gelation and polyelectrolyte complexation methods. Int. J. Pharm. 355, 299–306.

Shoaib, M.H., Tazeen, J., Merchant, H.A., Yousuf, R.I., 2006. Evaluation of drug release kinetics from ibuprofen matrix tablets using HPMC. Pak. J. Pharm. Sci. 19, 119–124.

Siepmanna, J., Peppas, N.A., 2000. Modeling of drug release from delivery systems based on hydroxypropyl methylcellulose (HPMC). Adv. Drug Deliv. Rev. 48, 139–157.

Singla, A.K., Chawla, M., 2001. Chitosan: some pharmaceutical and biological aspects—an update. J. Pharm. Pharmacol. 53, 1047–1067.

Trapani, A., Sitterberg, J., Bakowsky, U., Kissel, T., 2009. The potential of glycol CS-NPs as carrier for low water soluble drugs. Int. J. Pharm. 375, 97–106.

Wang, X., Chi, N., Tang, X., 2008. Preparation of estradiol CS-NPs for improving nasal absorption and brain targeting. Eur. J. Pharm. Biopharm. 70, 735–740.

Wu, Y., Yang, W., Wang, C., Hu, J., Fu, S., 2005. CS-NPs as a novel delivery system for ammonium glycyrrhizinate. Int. J. Pharm. 295, 235–245.

Xua, P., Van Kirk, E.A., Li, S., Murdoch, W.J., Ren, J., Hussain, M.D., Radosz, M., Shen, Y., 2006. Highly stable core-surface-crosslinked nanoparticles as cisplatin carriers for cancer chemotherapy. Colloids Surf. B 48, 50–57.

Zhang, L., Jiang, H., Zhu, W., Wu, L., Song, L., Wu, Q., Ren, Y., 2008. Improving the stability of insulin in solutions containing intestinal proteases in vitro. Int. J. Mol. Sci. 9, 2376–2387.

Zuo, Z., Kwon, G., Stevenson, B., Diakur, J., Wiebe, L.I., 2000. Flutamide–hydroxypropyl-β-cyclodextrin complex: formulation, physical characterization, and absorption studies using the Caco-2 in vitro model. J. Pharm. Pharm. Sci. 3, 220–227.